miRNA profiling of primate cervicovaginal lavage and extracellular vesicles reveals miR-186-5p as a potential retroviral restriction factor in macrophages

Zezhou Zhao[1], Dillon C. Muth[1], Kathleen Mulka[1], Zhaohao Liao[1], Bonita H. Powell[1], Grace V. Hancock[1,&], Kelly A. Metcalf Pate[1], Kenneth W. Witwer[1,2,*]

[1] Department of Molecular and Comparative Pathobiology, The Johns Hopkins University School of Medicine, 733 N. Broadway, Baltimore, MD 21218, USA; zzhao23@jhu.edu, dillon.muth@gmail.com, kmulka1@jhmi.edu, zliao1@jhmi.edu, bpowel15@jhu.edu, ghancock@ucla.edu, kpate5@jhmi.edu

[2] Department of Neurology; The Johns Hopkins University School of Medicine, 733 N. Broadway, Baltimore, MD 21218, USA; kwitwer1@jhmi.edu

[&] Currently at University of California, Los Angeles, Los Angeles, CA.

* Correspondence: kwitwer1@jhmi.edu; Tel.: +1-(410)-955-9770

Abstract: The goal of this study was to characterize extracellular vesicles (EVs) and miRNAs of primate cervicovaginal lavage (CVL) during the menstrual cycle and simian immunodeficiency virus (SIV) infection, and to determine if differentially regulated CVL miRNAs might influence retrovirus replication. CVL and peripheral blood were collected from SIV-infected and uninfected macaques. EVs were enriched by stepped ultracentrifugation and characterized thoroughly. miRNA profiles were assessed with a medium-throughput stem-loop/hydrolysis probe qPCR platform and validated by single qPCR assays. Hormone cycling was abnormal in infected subjects, but EV concentration correlated with progesterone concentration in uninfected subjects. miRNAs were present predominantly in the EV-depleted CVL supernatant. Only a small number of CVL miRNAs were found to vary during the menstrual cycle or SIV infection. Among them was miR-186-5p, which was depleted in retroviral infection. In experiments with infected macrophages in vitro, this miRNA inhibited HIV replication. These results provide further evidence for the potential of EVs and small RNAs as biomarkers or effectors of disease processes in the reproductive tract.

Keywords: extracellular vesicle; exosome; microvesicle; microRNA; biomarker; HIV-1; cervicovaginal lavage; SIV; restriction factor

1. Introduction

The cervicovaginal canal is a potential source of biological markers for forensics investigations [1–4], reproductive tract cancers [5–7], and infections [8–10]. Cervicovaginal secretions may be collected by swab, tampon, or other methods, or secretion components may be liberated by a buffered wash solution and collected as cervicovaginal lavage (CVL). In addition to utility as biomarkers, constituents of cervicovaginal secretions, including proteins, certain microbes, and metabolites, exert function, for example by playing protective roles in wound healing [11] and against HIV-1 infection [12–22]. A large and important body of work has thus examined biomarker potential and functional roles of numerous entities in the cervicovaginal compartment.

Compared with secreted proteins, metabolites, and the microbiome, however, several components of cervicovaginal fluids are less well understood, including extracellular RNAs (exRNAs) and their carriers, such as extracellular vesicles (EVs) and ribonucleoprotein complexes (exRNPs). EVs are potential regulators of cell behavior in paracrine and endocrine fashion due to their reported abilities to transfer proteins, nucleic acids, sugars, and lipids between cells [23]. EVs comprise a wide array of double-leaflet membrane extracellular particles, including those of endosomal and cell-surface origin[24,25], and range in diameter from 30 nm to well over one micron (large oncosomes) [26]. EV macromolecular composition tends to reflect, but is not necessarily identical to, that of the cell of origin [27]. EVs have been isolated from most cells, as well as biological fluids [23,28], including cervicovaginal secretions of humans [29] and rhesus macaques [30].

microRNAs (miRNAs) are one of the most studied classes of exRNA. These noncoding RNAs average 22 nucleotides in length and, in some cases, fine-tune the expression of target transcripts [31,32]. Released from cells by several routes, miRNAs are among the most frequently examined biomarker candidates in biofluids and, along with some other RNAs, are reported to be transmitted via EVs [33–36]. miRNAs are found not only in EVs, but also in free Argonaute-containing protein complexes; the latter may outnumber the former, at least in blood [37,38]. Many miRNAs are also highly conserved [32], and abundant species typically have 100% identity in humans and nonhuman primates [39]. (For this reason, we will refer to hsa- (*Homo sapiens*) and mml- (*Macaca mulatta*) miRNAs without the species designation unless otherwise warranted by sequence disparity.) While miRNAs have been profiled in cervicovaginal secretions and menstrual blood, mostly in the forensics setting [4,40,41], their associations with EV and exRNP fractions require further study. A recent publication reported that EVs from healthy vaginal secretions inhibited HIV-1 infection [29]. Another report found that CVL EVs (styled "exosomes") were present at higher concentrations in cervical cancer, and that two miRNAs were also upregulated [5]. Our laboratory described a reduction of CVL EVs in a severe endometriosis case compared with reproductively healthy primates [30]. However, our study, along with others, was limited by the absence of molecular profiling of EV cargo [30].

Here, we performed targeted miRNA profiling of EV-enriched and -depleted fractions of CVL and vaginal secretions collected from healthy and retrovirus-infected rhesus macaques. We queried how CVL EVs and miRNAs are affected by the menstrual cycle, an important potential confounder of biomarker studies [42]. Similarly, we assessed possible associations with simian immunodeficiency virus (SIV) infection. We report an association of miR-186 levels with SIV infection and find that this miRNA also appears to have antiretroviral effects in HIV-infected macrophages. These studies provide baseline information for easily accessed CVL markers including EVs and miRNAs that may become useful tools in the clinic.

2. Materials and Methods

Sample Collection

CVL and whole blood samples were collected weekly for five weeks from two uninfected (control) and four SIVmac251-infected (infected) rhesus macaques (*Macaca mulatta*) as previously described [30]. All macaques were negative for simian T-cell leukemia virus and simian type D retrovirus and were inoculated intravenously. Animals were sedated with ketamine at a dose of 7-10 mg/kg prior to all procedures. CVL was performed by washing the cervicovaginal cavity with 3 mL of phosphate buffered saline (PBS, Thermo Fisher Scientific, Waltham, MA, USA. Cat #: 14190-144) directed into the cervicovaginal canal and re-aspirated using the same syringe. Materials and procedures for sample collection are depicted in Supplemental Figure 1. Volumes of CVL yield across collection dates were documented in Supplemental Table 1. Whole blood (3 mL) was collected by venipuncture into syringes containing acid citrate dextrose solution (ACD) (Sigma Aldrich, St. Louis, MO, USA. Cat #: C3821).

Study Approvals

All animal studies were approved by the Johns Hopkins University Institutional Animal Care and Use Committee (IACUC) and conducted in accordance with the Weatherall Report, the Guide for the Care and Use of Laboratory Animals, and the USDA Animal Welfare Act.

Sample Processing

Sample processing began within a maximum of 60 minutes of collection and utilized serial centrifugation steps to enrich EVs as described previously [30], based on a standard EV isolation protocol [43]. Specifically, fluids were centrifuged: (1) 1,000 × *g* for 15mins at 4°C in a tabletop centrifuge; (2) 10,000 × *g* for 20 mins at 4°C; and (3) 110,000 × *g* for 2 hours at 4°C with a Sorvall Discovery SE ultracentrifuge (Thermo Fisher Scientific) with an AH-650 rotor (k factor: 53.0) (Supplemental Figure 1B). Following each centrifugation step, most supernatant was removed, taking care not to disturb the pellet. After each step, supernatant was set aside for nanoparticle tracking analysis (NTA; 200 μL), and RNA isolation (200 μL) following the second and third steps. The pellet was resuspended in 400 μL of PBS after each centrifugation step. After the final step, the remaining ultracentrifuged supernatant was concentrated to approximately 220 μL using Amicon Ultra-2 10 kDa molecular weight cutoff filters (Merck KGaA, Darmstadt, Germany. Cat #: UFC201024). 200 μL of the concentrate was used for RNA isolation and the remainder was retained for NTA. All samples reserved for RNA isolation were mixed with 62.6 μL of RNA isolation buffer (Exiqon, Vedbaek, Denmark. Cat #: 300112. Lot #: 593-84-9n) containing three micrograms of glycogen and 5 pg of synthetic cel-miR-39 as previously described [44]. Processed samples were analyzed immediately or frozen at -80°C until further use.

For plasma, whole blood was centrifuged at 800 × *g* for 10 mins at 25°C. Supernatant was centrifuged twice at 2,500 × *g* for 10 mins at 25°C. The resulting platelet-poor plasma was aliquoted and frozen at -80°C.

Hormone Analysis

Levels of progesterone (P4) and estradiol-17b (E2) were measured in plasma samples shipped overnight on dry ice to the Endocrine Technology and Support Core Lab at the Oregon National Primate Research Center, Oregon Health and Science University.

Nanoparticle Tracking Analysis

Extracellular particle concentration was determined using a NanoSight NS500 NTA system (Malvern, Worcestershire, UK). Cervicovaginal lavage samples were diluted as needed and specified in Supplemental Table 2 to ensure optimal NTA analysis. At least five 20-second videos were recorded for each sample at a camera setting of 12. Data were analyzed at a detection threshold of two using NanoSight software version 3.0.

Western Blot

Western blot was used to detect the presence of EV protein markers and the absence of nucleoporin (nuclear marker) in CVL and enriched CVL EVs. 20 μL of samples from each fraction were lysed with 5 μL 1:1 mixture of RIPA buffer (Cell Signaling Technology, Danvers, MA. Cat #: 9806S) and protease inhibitor (Santa Cruz Biotechnology, Dallas, TX. Cat #: sc29131). 8 μL of Laemmli 4X sample buffer (BioRad, Hercules, CA. Cat #:161-0747 Lot #: 64077737) was added per sample, and 30 μL of each was loaded into a Criterion TGX 4-15% gel (BioRad, Hercules, CA. Cat #: 5678084 Lot #: 64301319) after 5 mins of 95 °C incubation. The gel was electrophoresed by application of 100V for 100 mins. The proteins were then transferred to a PVDF membrane (BioRad, Hercules, CA. Cat #: 1620177, Lot #:31689A12.), which was blocked with 5% milk (BioRad, Hercules, CA. Cat #: 1706404. Lot #: 64047053) in PBS+0.1%Tween®20 (Sigma-Aldrich, St. Louis, MO Cat #: 274348 Lot #: MKBF5463V) for 1 hour. The membrane was subsequently incubated with mouse anti-human CD63 (BD Biosciences, San Jose, CA Cat #: 556019 Lot #: 6355939) and mouse monoclonal IgG_2b CD81 (Santa Cruz Biotechnology, Dallas, TX Cat #: 166029 Lot #: L1015) primary antibodies, at a concentration of 0.5 μg/mL overnight. After washing the membrane, it was incubated with a goat anti-mouse IgG-HRP secondary antibody (Santa Cruz Biotechnology, Dallas, TX Cat #: sc-2005 Lot #: B1616) at a 1:5,000 dilution for 1 h. The membrane was then incubated with a 1:1 mixture of SuperSignal West Pico Stable Peroxide solution and Luminol Enhancer solution (Thermo Scientific, Rockford, IL Cat #: 34080 Lot #: SD246944) for 5 min. The membrane was visualized on Azure 600 imaging system (Azure Biosystems, Dublin, CA). The second blot was done in a reducing environment using 10mM DTT (Promega, Madison, WI Cat #: P1171 Lot #: 0000198991). Same procedures were followed with rabbit anti-human TSG101 (Cat #: ab125011 Lot #:GR180132-14), rabbit polyclonal anti-nucleoporin (Abcam, Cambridge, MA Cat #: ab96134 Lot #: GR22167-18) primary antibodies. Subsequent incubation with goat anti-rabbit IgG-HRP secondary antibody (Abcam, Cambridge, MA Cat #: sc-2204 Lot #: B2216). All antibodies were used at the same concentration as the first blot. Membrane was visualized on the Azure imaging system.

Single particle interferometric reflectance imaging

Both CVL-derived and dendritic cell LK23-derived EVs were diluted 1:1000 and incubated on ExoView (NanoView Biosciences, Brighton, MA) chips that were printed with anti-CD63 (BD Biosciences, Bedford, MA. Cat#: 556019) and anti-CD81 (BD Biosciences, Bedford, MA. Cat #: 555675) antibodies. After incubation for 16 hours, chips were washed per manufacturer's protocol and imaged in the ExoView scanner by interferometric reflectance imaging.

Electron Microscopy

Gold grids were floated on 2% paraformaldehyde-fixed CVL–derived samples for two minutes, then negatively stained with uranyl acetate for 22 seconds. Grids were observed with a Hitachi 7600 transmission electron microscope in the Johns Hopkins Institute for Basic Biomedical Sciences Microscope Facility.

Total RNA Isolation and Quality Control

RNA isolation work flow is shown in Supplemental Figure 1C. RNA lysis buffer was added into each sample as described above prior to freezing (-80 °C). Total RNA was isolated from thawed samples using the miRCURY RNA Isolation Kit-Biofluids (Exiqon, Vedbaek, Denmark. Cat #: 300112. Lot #: 593-84-9n) per manufacturer's protocol with minor modifications as previously described[44]. Total RNA was eluted with 50 μL RNase-free water and stored at -80°C. As quality control, expression levels of several small RNAs including snRNA U6, miR-16-5p, miR-223-3p, and the spiked-in synthetic cel-miR-39 were assessed by TaqMan miRNA assays (Applied Biosystems/ Life Technologies, Carlsbad, California, USA) [45].

miRNA Profiling by TaqMan Low-Density Array

A custom 48-feature TaqMan low-density array (TLDA) was ordered from Thermo Fisher, with features chosen based on results of a human CVL pilot study (GVH and KWW, unpublished data). Stem-loop primer reverse transcription and pre-amplification steps were conducted using the manufacturer's reagents as previously described [46] but with 14 cycles of pre-amplification. Real time quantitative PCR was performed with a QuantStudio 12K instrument (Johns Hopkins University DNA Analysis Facility). Data were collected using SDS software and Cq values extracted with Expression Suite v1.0.4 (Thermo Fisher Scientific, Waltham, MA USA). Raw Cq values were adjusted by a factor determined from the geometric mean of 10 relatively invariant miRNAs. The selection process for these invariant miRNAs was to 1) rank miRNAs by coefficient of variation; 2) remove miRNAs with high average Cq (>30), non-miRNAs, and those with low amplification score; 3) select the lowest-CV member of miRNA families (e.g., the 17/92 clusters); and 4) pick the top 10 remaining candidates by CV: let-7b-5p, -miR-21-5p , -27a-3p, -28-3p, -29a-3p, -30b-5p, -92a-3p, -197-3p, -200c-3p, and -320a-3p.

Individual RT-qPCR Assays

Individual TaqMan miRNA qPCR assays were performed as previously described [46] on all UC pellet samples from all animals across all weeks for miRs-19a-3p (Thermo Fisher Assay ID #000395), -186-5p (Thermo Fisher Assay ID #002285), -451a-5p (Thermo Fisher Assay ID #001105) , -200c-3p (Thermo Fisher Assay ID #002300), -222-3p (Thermo Fisher Assay ID #002276), -193b-3p (Thermo Fisher Assay ID #002367), -181a-5p (Thermo Fisher Assay ID #000480), -223a-3p (Thermo Fisher Assay ID #002295), -16-5p (Thermo Fisher Assay ID #000391), -106a-5p (Thermo Fisher Assay ID #002169), and -125b-5p (Thermo Fisher Assay ID #00449). We also measured miR-375-3p (Thermo Fisher Assay ID #00564), which was not included on the array. Data were adjusted to Cqs of miR-16-5p.

Blood Cell Isolation and Monocyte-Derived Macrophage Culture

Total PBMCs were obtained from freshly drawn blood from human donors under a Johns Hopkins University School of Medicine IRB-approved protocol (JHU IRB #CR00011400). Blood was mixed with 10% Acid Citrate Dextrose (ACD) (Sigma Aldrich, St. Louis, MO Cat #: C3821 Lot #: SLBQ6570V) with gentle mixing by inversion. Within 15 minutes of draw, blood was diluted with equal volume of PBS+ 2% FBS, gently layered onto room temperature Ficoll (Biosciences AB, Uppsala, Sweden Cat #:17-1440-03 Lot #: 10253776) in Sepmate-50 tubes (STEMCELL Technologies, Vancouver, BC, Canada Cat #: 15450 Lot #: 06102016) and centrifuged for 10 minutes at 1200 × *g*. Plasma and PBMC fractions were removed, washed in PBS+ 2% FBS, and pelleted at 300 × *g* for 8 minutes. Pellets from 5 tubes were combined by resuspension in 10 mL RBC lysis buffer (4.15 g NH_4Cl, 0.5 g $KHCO_3$, 0.15 g EDTA in 450 mL H_2O; pH adjusted to 7.2–7.3; volume adjusted to 500 mL and filter-sterilized); total volume was brought to 40 mL with RBC lysis buffer. After incubation at 37 °C for 5 mins, the suspension was centrifuged at 400 × *g* for 6 mins at room temperature. The cell pellet was resuspended in Macrophage Differentiation Medium with 20% FBS (MDM20) to a final concentration of 2×10^6 cells/mL. PBMCs were plated at 4×10^6 cells per well in 12-well plates and cultured in MDM20 for 7 days. One half of the total volume of medium was replaced on day 3. On day 7, cells were washed 3 times with PBS to remove non-adherent cells. The medium was replaced with Macrophage Differentiation Medium with 10% serum (MDM10) and cultured overnight prior to transfection.

miRNA Mimic Transfection

Differentiated macrophages were transfected with 50 nM miRNA-186-5p (Qiagen, Foster City, CA. Cat #: MSY0000456 Lot #: 286688176) using Lipofectamine 2000 (Invitrogen/Life Technologies, Carlsbad, CA Cat #: 11668-019 Lot #:1467572) diluted in OptiMEM Reduced Serum Medium (Gibco, Grand Island, NY Cat #: 31985-070 Lot #: 1762285). Controls included mock transfections and transfection of 50 nM double-stranded siRNA oligo labeled with Alexa Fluor 555 (Invitrogen, Fredrick, MD Cat #: 14750-100 Lot #: 1863892). Plates were incubated for 6 hours at 37 °C. After incubation, successful transfection was confirmed by examining uptake of labeled siRNA with an

230 Eclipse TE200 inverted microscope (Nikon Instruments, Melville, NY). Transfection medium was
231 removed. The plates were washed with PBS and refed with 2 mL fresh MDM10 medium.
232
233 **HIV Infection**
234 HIV-1 BaL stocks were generated from infected PM1 T-lymphocytic cells and stored at −80 °C.
235 24 hours after mimic or mock transfections, macrophages were infected with HIV BaL and incubated
236 overnight (stock, 80 μg p24/mL, diluted to 200 ng p24/mL). At days 3, 6, and 9 post-infection, 500 μL
237 supernatant was collected for p24 release assays and cells were lysed with 600 μL mirVana lysis buffer
238 for subsequent RNA isolation and analysis.
239
240 **HIV p24 Antigen ELISA**
241 Supernatant samples were lysed with Triton-X (Perkin Elmer, Waltham, MA Cat #:
242 NEK050B001KT Lot #: 990-17041) at a final concentration of 1%. The DuPont HIV-1 p24 Core Profile
243 ELISA kit (Perkin Elmer, Waltham, MA Cat #: NEK050B001KT Lot #: 990-17041) was used per
244 manufacturer's instructions to measure p24 concentration based on the provided standard.
245
246 **Total RNA Isolation**
247 Total RNA was isolated using the mirVana miRNA Isolation Kit per manufacturer's protocol
248 (Ambion, Vilnius, Lithuania. Cat #: AM1560 Lot #: 1211082). Note that this procedure yields total
249 RNA, not just small RNAs. After elution with 100 μL RNase-free water, nucleic acid concentration
250 was measured using a NanoDrop 1000 spectrophotometer (Thermo Fisher Scientific, Wilmington,
251 DE). RNA isolates were stored at -80 °C.
252
253 **HIV Gag RNA RT-qPCR**
254 Real-time one-step reverse transcription quantitative PCR was performed with the QuantiTect
255 Virus Kit (Qiagen, Foster City, CA Cat #:211011 Lot #: 154030803). Each 25 μl reaction mixture
256 contained 15 μl of master mix containing HIV-1 RNA standard, 100 μM of FAM dye and IBFQ
257 quencher labeled Gag probe (5′ ATT ATC AGA AGG AGC CAC CCC ACA AGA 3′), 600 nM each of
258 Gag1 forward primer (5′TCA GCC CAG AAG TAA TAC CCA TGT 3′) and Gag2 reverse primer (5′
259 CAC TGT GTT TAG CAT GGT GTT T 3′), nuclease-free water, and QuantiTect Virus RT mix, and 10
260 μL serial-diluted standard or template RNA. No-template control and no reverse transcriptase
261 controls were included. Linear standard curve was generated by plotting the log copy number versus
262 the quantification cycle (Cq) value. Log-transformed Gag copy number was calculated based on the
263 standard curve.
264
265 **Data analysis**
266 Data processing and analysis were conducted using tools from Microsoft Excel (geometric mean
267 normalization), Apple Numbers, GraphPad Prism, the MultiExperiment Viewer, and
268 R/BioConductor packages including pheatmap (http://CRAN.R-project.org/package=pheatmap;
269 quantile normalization, Euclidean distance, self-organizing maps, self-organizing tree algorithms, k-
270 means clustering). Figures and tables were prepared using R Studio, Microsoft Excel and Word,
271 Apple Numbers and Keynote, GraphPad Prism, and Adobe Photoshop.
272
273 **Data Availability and Rigor and Reproducibility**
274 Array data have been deposited with the Gene Expression Omnibus (GEO) [47] as GSE107856.
275 Data in other formats are available upon request. To the extent that sample quantities would allow,
276 the MISEV recommendations for EV studies were followed[24], and the EV experiments have been
277 registered with the EV-TRACK knowledgebase, [48] with preliminary EV-TRACK code XL5296IL.
278

3. Results

3.1. Abnormal menstrual cycle of SIV-infected macaques and ovulation-associated changes in CVL EV-enriched particles

Plasma and CVL were collected from two control and four SIV-infected macaques over the course of five weeks (Supplemental Figure 1). Abnormal cycling was observed for infected subjects (K. Mulka, et al, unpublished data). By nanoparticle tracking analysis, CVL EV concentration in control animals increased during ovulation (Figure 1A). Transmission electron microscopy was performed for representative fractions of CVL, revealing bacteria and large particles in the 10,000 × g pellet (Figure 1B). The 100,000 x g pellet included apparent EVs up to 200 nm in diameter (Figure 1C). EV markers (shown: CD63, CD81, and TSG101) were confirmed by Western blot (Figure 1D). The nuclear marker nucleoporin was detected only in tissue samples (Figure 1D). The relative EV tetraspanin profiles of both CVL and control EV samples were corroborated with single particle interferometric reflectance imaging: CVL EVs had a higher CD63 expression and dendritic cell EVs had higher CD81 expression.

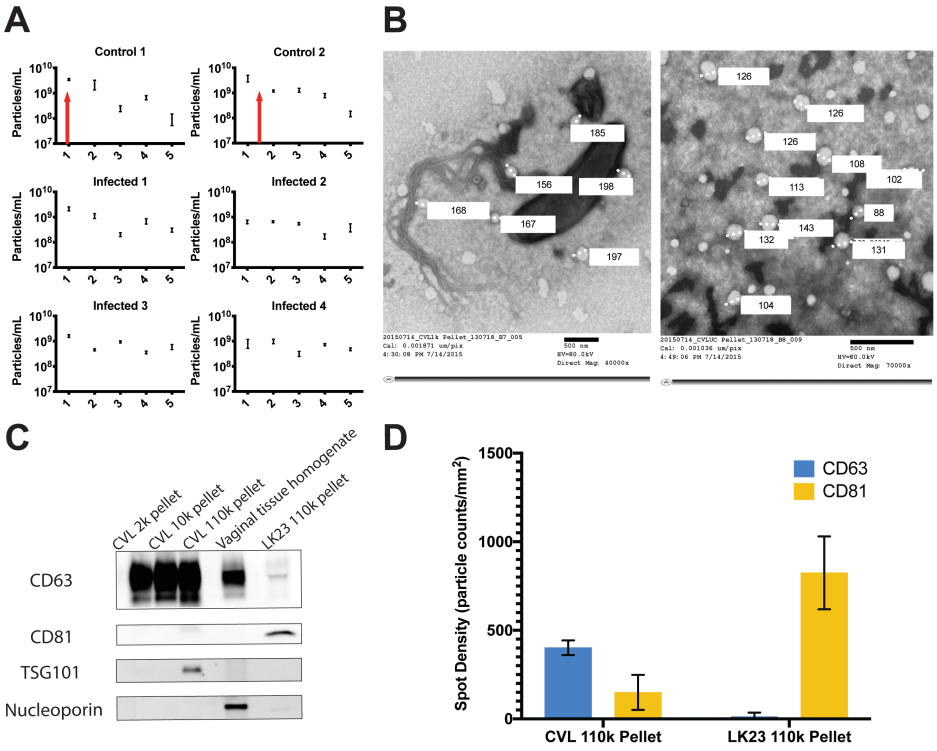

Figure 1. EV composition during the menstrual cycle. **A)** Nanoparticle concentrations of CVL ultracentrifuge (UC) pellets monitored weekly over five weeks for two SIV-negative ("control") and four SIV-infected rhesus macaques. Red arrows indicate time of ovulation for 2 control animals, which were absent for SIV infected animals. **B**) Transmission electron micrographs of CVL pellets from the 10,000× g pellet **(left)** and 110,000× g pellet **(right)** confirm presence of bacteria and EVs/EV-like particles, with several respective diameters indicated. **C)** Western blot analysis suggests enrichment of EV markers CD63, CD81, and TSG101 in 110k pellet fraction of CVL from uninfected animals. Vaginal tissue homogenate and dendritic cell (DC, LK23) 110k pellet controls were also positive for CD63 and CD81. Nuclear marker nucleoporin was detected in tissue homogenate but not in putative EV samples. **D)** SP-IRIS confirmation of EV markers on CVL and DC EVs. Shown are averages of tetraspanin-positive particles bound to anti-CD63 and anti-CD81 antibodies and detected by label-free imaging.

3.2. TLDA reveals an extracellular miRNA profile of the cervicovaginal compartment

307 Based upon preliminary findings from a study of human CVL (Hancock and Witwer,
308 unpublished data), we designed a custom TaqMan low-density array (TLDA) to measure 47 miRNAs
309 expected to be present in CVL, along with the snRNA U6. CVL from all subjects and at all time points
310 was fractionated by stepped centrifugation to yield a 10,000 x g pellet (10K pellet), a 100,000 x g pellet
311 (UC pellet), and 100,000 x g supernatant (UC supernatant). Total RNA from all fractions was profiled
312 by TLDA. Raw (Supplemental Figure S2A), quantile normalized (Supplemental Figure S2B), and
313 geometric mean-adjusted Cq values (Supplemental Figure S2C) were subjected to unsupervised
314 hierarchical clustering. This clustering did not reveal broad miRNA profile differences associated
315 with sample collection time, menstruation, or SIV infection.

316 *3.3. Distribution of miRNAs across CVL fractions*

317 Across the three examined CVL fractions (p10, p100, S100), the ten most abundant miRNAs
318 (lowest Cq values) were miRs-223-3p, -203a-3p, -24-3p, -150-5p, -21-5p, -146a-5p, -92a-3p, -222-3p, -
319 17-5p, and -106a-5p. The average normalized Cq value for each miRNA was greater (i.e., lower
320 abundance) in the p100 than the s100 fraction (Figure 2A and inset), and indeed in p10 and p100
321 combined (Figure 3B), suggesting that most miRNA in CVL, as reported for various other body fluids,
322 is found outside the EV-enriched fractions. Considering all fractions, the differences between the EV-
323 enriched and EV-depleted fractions were significant even after Bonferroni correction for all features
324 except U6. On average, the s100 fraction contained 86.5% of the total miRNA from these three
325 fractions. In the p10 fraction, the average miRNA was detected at 10.5% its level in the s100 fraction
326 (SD=5.7%). miR-34a-5p had the lowest (5.9%) and miR-28-3p the highest (33.7%) abundance
327 compared with s100. In the p100 fraction, miRNAs were on average 5.6% (SD=2.4%) as abundant as
328 in s100. The least represented in p100 was miR-27a-3p (2.3%), and the best represented was again
329 miR-28-3p (13.4%). Together, the content of the EV-enriched fractions (p10 and p100) as a percentage
330 of the total is shown in Figure 2B for individual miRNAs. miRNA rank was significantly correlated
331 across fractions, despite minor differences in order (Figure 2C).

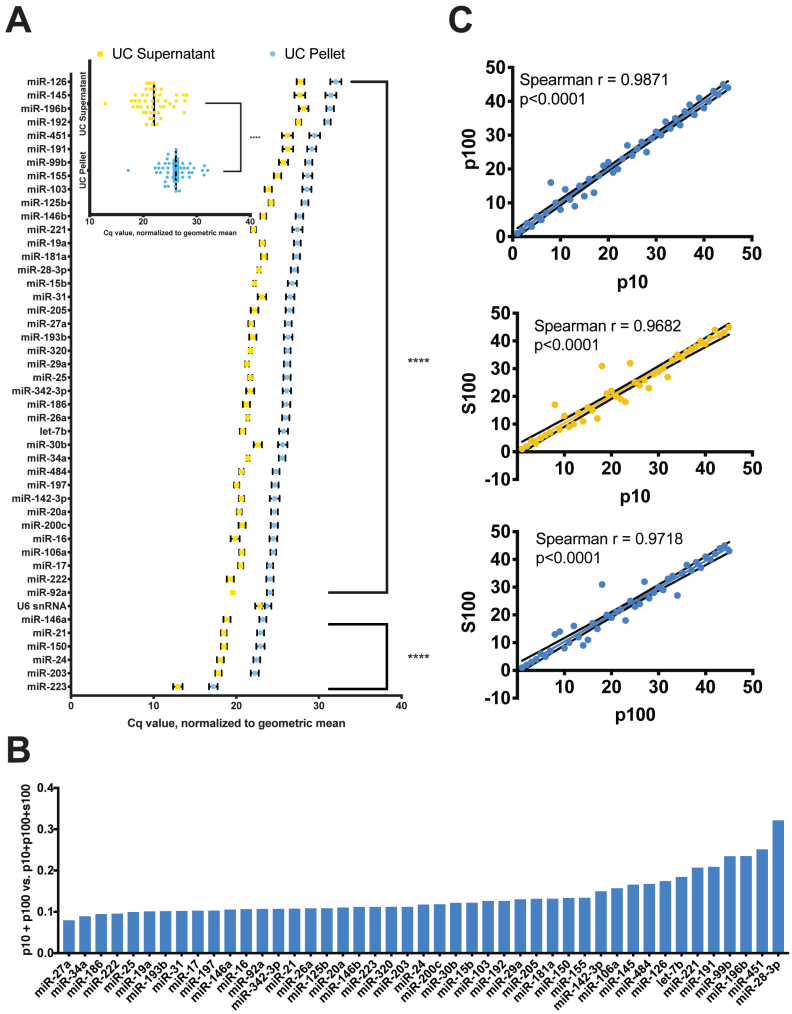

Figure 2. Relative abundance of miRNAs in different CVL fractions. **A)** Abundant miRNAs in descending order based on Cq values normalized to the geometric mean for each sample. Inset: average of all miRNAs in UC pellet and UC supernatant. Error bars: SEM. **B)** miRNA expression in EV-enriched fractions (p10, p100) as a percentage of total estimated expression (p10+p100+S100 by Cq) in ascending order, from miR-27a-3p (7.9%) to miR-28-3p (32.0%). **C)** miRNAs in each fraction (10,000× g pellet=p10, 110,000 × g pellet=p100, 110,000× g supernatant=S100, and) are significantly correlated (p<0.0001, Spearman).

3.4. qPCR Validation

Individual stem loop RT/hydrolysis probe qPCR assays were used to verify TLDA results for eleven selected miRNAs plus miR-375-3p (not included on the array), which was also measured because of a reported association with goblet cells [49]. Some miRNAs were chosen due to high expression levels. miR-181a-5p was measured due to its association with endometrial cells [50,51]. miR-125b-5p has been reported as a diagnostic marker of endometriosis [52]. Other miRNAs (miRs-186-5p, -451a-5p, -200c-3p, -222-3p, -193b-3p) were selected based on our previous experience and results from other studies evaluating miRNAs in the context of HIV-1 and SIV infections. Results of qPCR assays, adjusted by miR-16-5p for each sample (since we found relatively low qPCR variation of miR-16-5p, a commonly used normalizer [53]), are shown in Figure 3A. Figure 3B compares miRNA ranks (1-11) by TLDA and individual qPCR, which are generally in concordance. Note that expression of red blood cell miRNA miR-451a-5p was low, suggesting minimal contamination from blood for most samples.

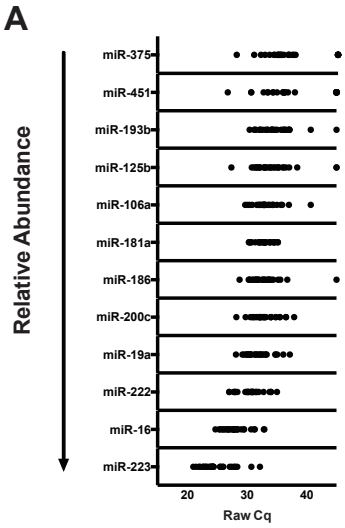

B

Relative Abundance Rank by qPCR	miRNA	Rank of Relative Abundance by TLDA
1	hsa-miR-223-3p	1
2	hsa-miR-16-5p	3
3	hsa-miR-222-3p	2
4	hsa-miR-19a-3p	9
5	hsa-miR-200c-3p	4
6	hsa-miR-186-5p	6
7	hsa-miR-181a-5p	8
8	hsa-miR-106a-5p	5
9	hsa-miR-125b-5p	10
10	hsa-miR-193b-3p	7
11	hsa-miR-451a-5p	11

Figure 3. miRNA qPCR validation. **A)** qPCR validation for UC pellet samples, all subjects and time points (individual dots). **B)** Ranks of abundant miRNAs by qPCR and TLDA.

3.5.miRNA association with retroviral infection status

An association of miRNA abundance with infection status could yield novel biomarkers as well as clues to roles of miRNA in modulating infection. However, the small number of subjects in our study was a challenge. Nevertheless, by considering all subjects and time points together for both infected and uninfected subjects, microarray data suggested a slightly reduced abundance of miRs-186-5p, -222-3p, and -200c-3p in infected samples (Figure 4A) based on statistical analysis of ΔCq values, while qPCR revealed differential abundance of miRs-186-5p and -125b-5p (Figure 4B). miR-186-5p was thus identified by both techniques as potentially associated with retroviral infection.

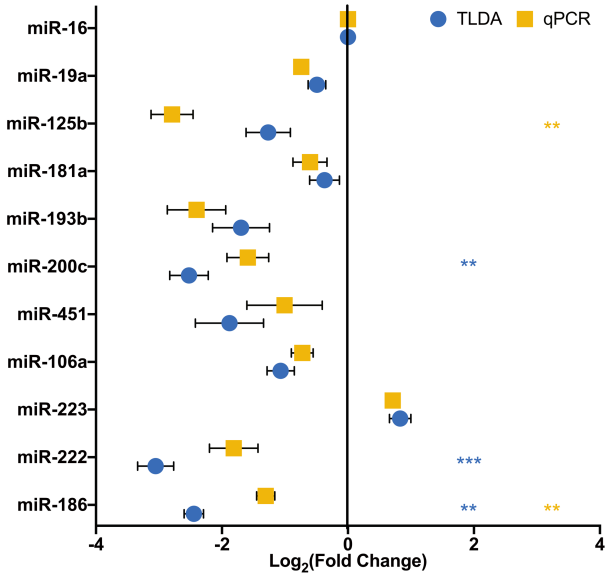

Figure 4. miR-186-5p downregulation: SIV. miR-186-5p fold change was determined using $\Delta\Delta Ct$ method using miR-16 and uninfected animals as controls. $Log_2(fold\ change)$ for both TLDA and qPCR analyses was plotted for 11 selected validation miRNAs. Statistical analyses were performed on ΔCt values. For TLDA, miRs-186, -222, and -200c were significantly less abundant in the CVL p100 fraction of infected subjects (Mean ± SEM, Multiple t test, Bonferroni-Dunn Correction), ** $p < 0.01$, *** $p<0.001$. For qPCR analysis, miRs-186 and -125b were significantly less abundant (Multiple t test, Bonferroni-Dunn Correction), ** $p < 0.01$, *** $p<0.001$

372 *3.6. miR-186-5p transfection has minimal effects on cellular HIV RNA abundance but reduces p24 release*
373 *from monocyte-derived macrophages*

374 To assess a possible influence of miR-186-5p ("miR-186") on retroviral replication, we
375 introduced double-stranded miR-186-5p mimic or control RNA into monocyte-derived macrophages
376 derived from three donors 24 hours before infecting the cells or not with HIV. At days three and six
377 post-infection, we quantitated full-length HIV-1 transcript using a gag qPCR with standard curve. In
378 cells from only one of three donors were fewer HIV-1 copies associated with miR-186-5p mimic
379 transfection (Figure 5). Overall, there was no statistically significant difference in HIV RNA between
380 the conditions.

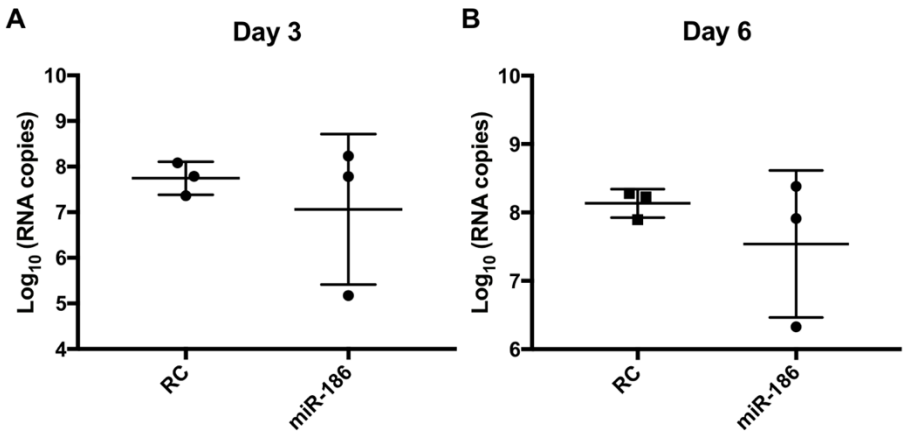

381

382 **Figure 5.** miRNA-186-5p mimic transfection inconsistently suppresses HIV-1 gag mRNA production.
383 Apparent downregulation of gag mRNA (qPCR assay with standard curve) was observed in miR-
384 186-transfected monocyte-derived macrophages from only 1 of 3 donors compared with control RNA-
385 transfected cells (RC). Overall, results were insignificant by t-test, $p>0.1$, with multiple replicates of
386 cells from 3 human donors.

387 However, at the same time points and also out to nine days post-infection, a different result was
388 seen for capsid p24 release into the supernatant. For infected but untransfected cells, measurable p24
389 was observed by 3 dpi, and p24 counts increased by two-fold or more by 9 dpi (Figure 6A) for
390 multiple replicate experiments with cells from three donors. Compared with infected, untreated
391 controls, mock-transfected cells (not shown), and cells transfected with a negative control RNA
392 (labeled with a fluorophore to assess transfection efficiency), miR-186-5p transfection was associated
393 with a significant decline of released p24 at all time points (ANOVA with Bonferroni correction)
394 (Figure 6B-D). The negative control condition showed a suppressive trend that reached nominal
395 significance at 9 dpi. However, miR-186-associated suppression was significantly greater at all time
396 points.

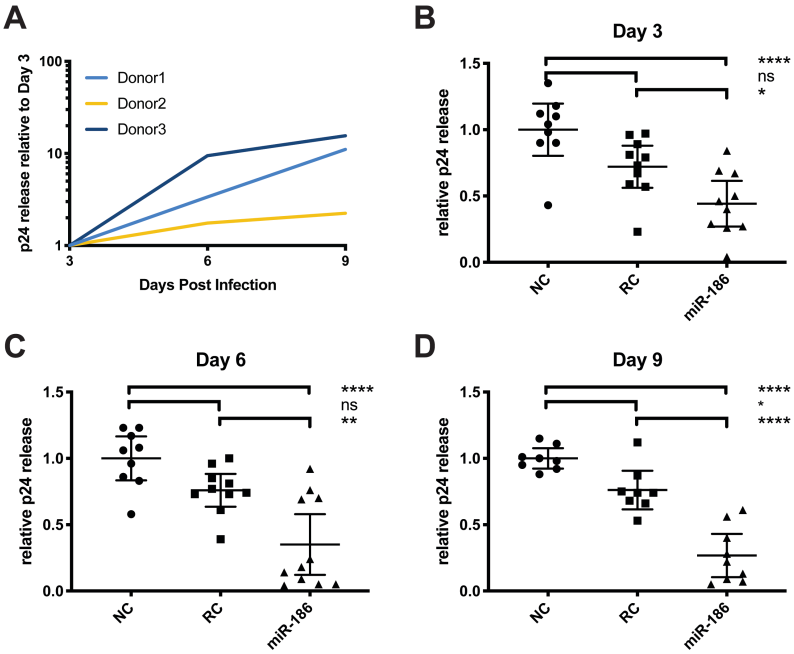

Figure 6. miRNA-186-5p inhibits p24 release. Monocyte-derived macrophages from human donors were infected with HIV-1 BaL. **A)** p24 production increased >2 fold for all donors from 3 to 9 days post-infection (dpi), untreated cells. **B-D)** Transfection of miR-186-5p mimic was associated with a decrease of p24 release compared with untransfected controls (NC) and control RNA mimic-transfected controls (RC) at the indicated time points; ns=not significant, * $p<0.05$, ** $p<0.01$, **** $p<0.0001$ (ANOVA followed by Bonferroni correction for multiple tests). Results were from 8 to 11 replicate experiments with cells from 3 human donors.

3.7 p24 inhibition by miR-186-5p is correlated with transfection efficiency

Despite the statistical significance of miR-186-5p-associated p24 inhibition, substantial variability was observed, including between donors/experiments; we therefore hypothesized that either donor- or experiment-specific factors were responsible for the variability. The transfection experiments were repeated using macrophages from five additional donors (labeled 1-5). While significant but variable inhibition of p24 release after miR-186-5p transfection was observed for three donors (1, 2, and 5), little or no inhibition was seen for donors 3 and 4 (Figure 7).

One experimental variable that could affect the degree of inhibition is the efficiency with which the miRNA mimic is delivered into the cells. Since this variable was not assessed in our previous experiments, we measured it for the five new experiments. Despite using the same nominal concentrations of miRNA mimics for our experiments, a nearly 100-fold range of miR-186-5p concentration was observed between the lowest- and highest-efficiency transfections (Figure 9A), which increased miR-186-5p levels from around 5-fold to nearly 500-fold, respectively. Strikingly, the miR-186-5p level was inversely correlated with released p24 across these five donors. It should be noted that miR-186-5p antisense inhibitors were also introduced in these experiments. While they did not significantly increase HIV p24 release (Figure 7), they also did not achieve a consistent knockdown of native miR-186-5p (Figure 8A).

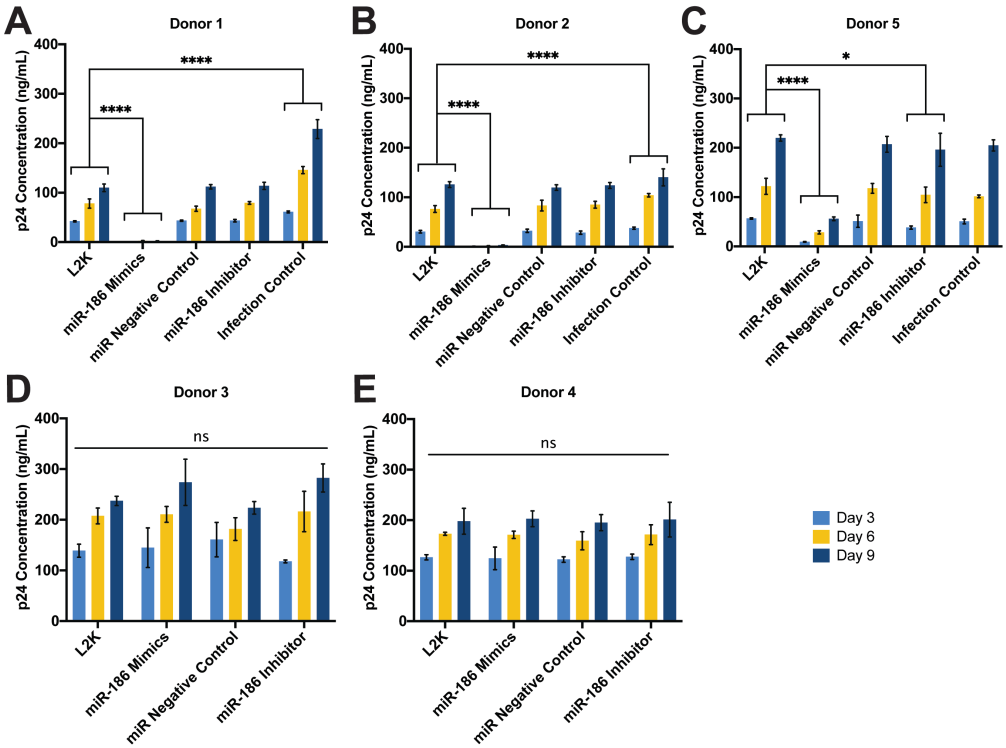

Figure 7. miRNA-186-5p inhibits p24 release in a donor-specific manner. Monocyte-derived macrophages from human donors were infected with HIV-1 BaL. **A-C)** Compared with mock transfected controls, transfection of miR-186 mimic was associated with a significant decrease of p24 production from 3 to 9 days post-infection (dpi) in donors 1, 2, and 5. **D-E)** For donors 3 and 4, transfection of miR-186 mimic was ineffective in inhibiting p24 release compared with mock transfected controls; ns=not significant, * p<0.05, ** p<0.01, **** p<0.0001 (Two-way ANOVA followed by Bonferroni correction for multiple tests).

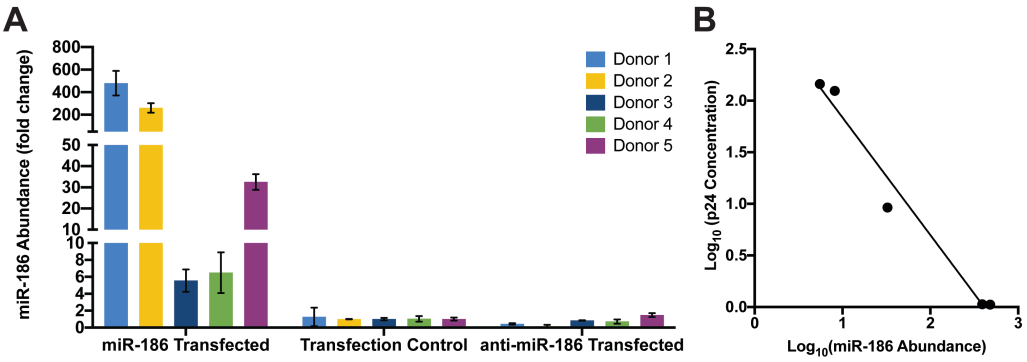

Figure 8. miR-186-5p abundance post-transfection and correlation with p24 release. **A)** Abundance of miR-186-5p in macrophages post-transfection, as assessed by qPCR and compared (fold change) with the average of control macrophages. **B)** Correlation of macrophage miR-186-5p and p24 concentration released in supernatant three days post-infection. p(two-tailed)=0.0019 (Correlation), $R^2 = 0.9731$(Linear regression).

4. Discussion

Cervicovaginal lavage EVs and exRNPs, like EVs in the uterus [54,55], may offer information about the health of the reproductive tract and may also facilitate or block transmission of infectious agents. Proteomic analyses of human [56] and rhesus macaque [57] CVL have suggested a core proteome and a highly variable proteome that responds to changes in pregnancy status, menstruation, infection, and other stressors. However, exRNA and extracellular vesicle profiles are less understood in this compartment. Thus, one major finding of this study is a partial profile of miRNAs of EV-enriched and -depleted fractions of CVL fluid of primates. We report that EVs can be liberated from vaginal secretions by lavage, and that these EVs can be concentrated using a standard stepped centrifugation procedure, with enrichment of positive (membrane-associated) markers while a cellular negative control was not detected.

Both EV-replete and EV-depleted fractions of CVL contained abundant miRNA. As reported for other biological fluids [37,58], miRNA concentration was highest in the EV-depleted CVL fractions, not in EV-enriched ultracentrifuged pellets, consistent with packaging of most extracellular miRNA into exRNPs; the function, if any, of extracellular miRNAs in the cervicovaginal tract of healthy individuals remains to be determined. We observed minimal differences in extracellular miRNA profiles between SIV-infected and uninfected subjects or, surprisingly, even during the menstrual cycle, suggesting a certain stability of extracellular miRNA in the compartment. Correlation of miRNA concentrations in EV-depleted and -replete fractions was also apparent. Based on relative abundance compared with miRNAs of other cellular/tissue origins (e.g., heart and lung specific miR-126, kidney-specific miR-196b, and liver-specific miR-192) [59,60], miRNAs in EVs and exRNPs of CVL are likely derived from epithelial cells (including goblet cells), and cells of the immune system (as suggested, e.g., by myeloid-enriched miR-223 and lymphocyte-enriched miR-150)[61]. Of the most abundant miRNAs we identified, some have been ascribed tumor-suppressive roles in cancers[62–68]. Also, miR-223 and miR-150 have been described as "anti-HIV" miRNAs [69] among a variety of reported antiretroviral small RNAs (sRNAs), both host and viral [70–75]. Given their relative abundance in the vaginal tract, a common site for HIV infection, these miRNAs may contribute to antiviral defenses.

Along these lines, a second major finding of this study is a possible role for miR-186-5p in antiretroviral defense, bolstered by the observation that exogenous miR-186-5p transfection efficiency correlates inversely with HIV p24 release. Previous publications have identified protein constituents in the cervicovaginal lavage with anti-HIV efficacies (for example [7,14,22]). Our identification of miRNA as a potential anti-HIV agent adds an element of complexity to the picture of tissue-specific antiretroviral defense. In contrast with an early report of direct binding of host miRNAs to retroviral transcripts and subsequent suppression [69], it now appears that this mechanism of suppression may be relatively uncommon [76]. Anti-HIV miRNAs may be more likely to exert effects through control of host genes instead (e.g., [77]). Our data also support the conclusion that reduction of HIV RNA levels is not the main mechanism for miR-186-mediated suppression of HIV release.

How, then, might miR-186-5p, whether endogenous or exogenous (therapeutically introduced) contribute to antiretroviral effects? Combining several miRNA target prediction, validation, and enrichment analysis approaches [78–84], we noticed a few putative miR-186-5p targets and related pathways that may merit follow-up. One target of miR-186-5p that was validated experimentally by multiple methods is FOXO1 [85], an important contributor to apoptosis but also immunoregulation via IFNγ pathways. Another prominent validated target, P2X7R [86], is involved in membrane budding, T-cell-mediated cytotoxicity, cellular response to extracellular stimuli and T-cell homeostasis/proliferation. There is also evidence that miR-186-5p targets the HIV co-receptor CXCR4 [87]. Pathway enrichment analyses [83,84] suggest that miR-186-5p targets participate significantly in infection-related networks, including prion diseases, viral carcinogenesis, and responses to measles and herpes simplex virus infections. Although miRNA target prediction algorithms are imperfect, and validation efforts are of varying quality [88,89], these findings may shed some light on how miR-186-5p is involved in responses to HIV.

We would like to emphasize several aspects of the study that open the door to future research:

491 1. We used stepped ultracentrifugation without density gradients because of the small sample
492 volumes available. Although stepped ultracentrifugation remains a widely used method for EV
493 enrichment [43,90], subsequent gradients or alternative isolation methods could be attempted with
494 larger volume samples to increase purity in future. Possibly, our study overestimates the
495 abundance of miRNAs in CVL EVs, and differential packaging into EVs and exRNPs is masked
496 by contamination of our EV preps with exRNPs.

497 2. Our qPCR array approach and focus on miRNAs leaves room for additional work. While we
498 are confident that our array captured most of the abundant miRNAs in CVL, sequencing short
499 and longer RNAs could reveal additional markers.

500 3. The small number of subjects and the absence of obvious menstrual cycle in infected subjects
501 precludes strong conclusions about EV or miRNA associations with either infection or the
502 menstrual cycle. For example, we did not observe the expected increase in miR-451a or other
503 red blood cell-specific miRNAs during menstruation. However, since only two animals showed
504 evidence of cycling, experiments with more subjects and larger sample volumes are needed.

505 4. Our previous criticisms of miRNA functional studies [91] also apply to our results here.
506 Additional work is needed to assess the potential of miR-186-5p to regulate retrovirus
507 production at endogenous levels, for example by showing that it is present in active RNPs [92]
508 and that it interacts directly with specific host or viral targets. However, it is also important to
509 note that miR-186-5p could have therapeutic benefit even if it must be delivered at
510 supraphysiologic concentrations. Finally, it is possible, but must be demonstrated, that miR-
511 186-5p acts in a paracrine fashion via EV or exRNP shuttles.

512 5. We have investigated the effects of miR-186-5p only in monocyte-derived macrophages. We
513 chose to begin with this cell type because of the abundance of miR-223 and the known role of
514 macrophages in the epithelium. Other cell types should also be investigated.

515 Overall, the results presented here support further development of CVL and its constituents as a
516 window into the health of the cervicovaginal compartment in retroviral infection and beyond.
517 Furthermore, delivery of miR-186-5p could act to suppress retrovirus release.

518

Supplementary Materials: Figure S1: Specimen Collection and Sample Processing Workflow, Figure S2: miRNA profile of CVL fractions, Table S1: Recovered volumes: CVL, Table S2: NTA dilution factors, CVL, Table S3: Pooling Strategy

Author Contributions: Conceptualization, Zezhou Zhao, Dillon C. Muth, Grace V. Hancock, Kelly A. Metcalf Pate and Kenneth W. Witwer; Data curation, Zezhou Zhao and Kenneth W. Witwer; Formal analysis, Zezhou Zhao, Dillon C. Muth and Kenneth W. Witwer; Funding acquisition, Kenneth W. Witwer; Investigation, Zezhou Zhao, Dillon C. Muth, Kathleen Mulka, Zhaohao Liao and Bonita H. Powell; Methodology, Zezhou Zhao, Kathleen Mulka, Grace V. Hancock, Kelly A. Metcalf Pate and Kenneth W. Witwer; Project administration, Kenneth W. Witwer; Resources, Kelly A. Metcalf Pate and Kenneth W. Witwer; Supervision, Zhaohao Liao and Kenneth W. Witwer; Visualization, Zezhou Zhao, Dillon C. Muth and Kenneth W. Witwer; Writing – original draft, Kenneth W. Witwer; Writing – review & editing, Zezhou Zhao, Dillon C. Muth and Kenneth W. Witwer.

Funding: This research was funded by the Johns Hopkins University Center for AIDS Research, an NIH funded program, grant number P30AI094189 (pilot grant to KWW; ZZ and GVH were Baltimore HIV/AIDS scholars); by the US National Institutes of Health, DA040385, DA047807, AI144997, and MH118164 (to KWW); by UG3CA241694, supported by the NIH Common Fund, through the Office of Strategic Coordination/Office of the NIH Director; and by the National Center for Research Resources and the Office of Research Infrastructure Programs (ORIP) and the National Institutes of Health, grant number P40 OD013117. DM and KM received support through NIH grant number T32 OD011089.

Acknowledgments: The authors thank Robert Adams, Lauren Ostrenga, and Sarah Beck for contributions to these studies. The authors gratefully acknowledge the Oregon National Primate Research Center and David Erikson for hormone analyses and endocrinology advice and thank Barbara Smith of the JHU IBBS Microscope Facility for expert assistance with electron microscopy. Amanda Steele provided paid assistance with editing and organizing an early version of the manuscript.

Conflicts of Interest: The authors have no competing interests to declare. The funding organization(s) played no role in the study design; in the collection, analysis, and interpretation of the data; in the writing of the report; or in the decision to submit the report for publication.

546 **REFERENCES**

547 1. Hanson EK, Ballantyne J. Highly specific mRNA biomarkers for the identification of vaginal
548 secretions in sexual assault investigations. *Sci Justice*. 2013;53(1):14-22.
549 doi:10.1016/j.scijus.2012.03.007

550 2. Jakubowska J, MacIejewska A, Pawłowski R, Bielawski KP. MRNA profiling for vaginal fluid
551 and menstrual blood identification. *Forensic Sci Int Genet*. 2013;7(2):272-278.
552 doi:10.1016/j.fsigen.2012.11.005

553 3. Park JL, Kwon OH, Kim JH, et al. Identification of body fluid-specific DNA methylation
554 markers for use in forensic science. *Forensic Sci Int Genet*. 2014;13:147-153.
555 doi:10.1016/j.fsigen.2014.07.011

556 4. Hanson EK, Lubenow H, Ballantyne J. Identification of forensically relevant body fluids using
557 a panel of differentially expressed microRNAs. *Anal Biochem*. 2009;387(2):303-314.
558 doi:10.1016/j.ab.2009.01.037S0003-2697(09)00065-7 [pii]

559 5. Liu J, Sun H, Wang X, et al. Increased Exosomal MicroRNA-21 and MicroRNA-146a Levels in
560 the Cervicovaginal Lavage Specimens of Patients with Cervical Cancer. *Int J Mol Sci Int J Mol*
561 *Sci*. 2014;15:758-773. doi:10.3390/ijms15010758

562 6. Van Ostade X, Dom M, Tjalma W, Van Raemdonck G. Candidate biomarkers in the cervical
563 vaginal fluid for the (self-)diagnosis of cervical precancer. *Arch Gynecol Obstet*. 2018;297(2):295-
564 311. doi:10.1007/s00404-017-4587-2

565 7. Van Raemdonck GAA, Tjalma WAA, Coen EP, Depuydt CE, Van Ostade XWM. Identification
566 of Protein Biomarkers for Cervical Cancer Using Human Cervicovaginal Fluid. *PLoS One*.
567 2014;9(9):e106488. doi:10.1371/journal.pone.0106488

568 8. Gravett MG, Thomas A, Schneider KA, et al. Proteomic Analysis of Cervical−Vaginal
569 Fluid: Identification of Novel Biomarkers for Detection of Intra-amniotic Infection. *J Proteome*
570 *Res*. 2007;6(1):89-96. doi:10.1021/pr060149v

571 9. Datcu R, Gesink D, Mulvad G, et al. Bacterial vaginosis diagnosed by analysis of first-void-
572 urine specimens. *J Clin Microbiol*. 2014;52(1):218-225. doi:10.1128/JCM.02347-13

573 10. Srinivasan S, Morgan MT, Fiedler TL, et al. Metabolic signatures of bacterial vaginosis
574 Supplementary file: Figure S1. *MBio*. 2015;6(2):1-16. doi:10.1128/mBio.00204-15

575 11. Zevin AS, Xie IY, Birse K, et al. Microbiome Composition and Function Drives Wound-
576 Healing Impairment in the Female Genital Tract. *PLoS Pathog*. 2016;12(9):e1005889.
577 doi:10.1371/journal.ppat.1005889

578 12. Boggiano C, Littman DR. HIV's Vagina Travelogue. *Immunity*. 2007;26(2):145-147.
579 doi:10.1016/j.immuni.2007.02.001

580 13. Patel M V., Ghosh M, Fahey J V., Ochsenbauer C, Rossoll RM, Wira CR. Innate Immunity in
581 the Vagina (Part II): Anti-HIV Activity and Antiviral Content of Human Vaginal Secretions.
582 *Am J Reprod Immunol*. 2014;72(1):22-33. doi:10.1111/aji.12218

583 14. Burgener A, Boutilier J, Wachihi C, et al. Identification of differentially expressed proteins in
584 the cervical mucosa of HIV-1-resistant sex workers. *J Proteome Res*. 2008;7(10):4446-4454.
585 doi:10.1021/pr800406r

586 15. Benki S, Mostad SB, Richardson BA, Mandaliya K, Kreiss JK, Overbaugh J. Increased levels of
587 HIV-1-infected cells in endocervical secretions after the luteinizing hormone surge. *J Acquir*
588 *Immune Defic Syndr*. 2008;47(5):529-534. doi:10.1097/QAI.0b013e318165b952

589 16. Zara F, Nappi RE, Brerra R, Migliavacca R, Maserati R, Spinillo A. Markers of local immunity
590 in cervico-vaginal secretions of HIV infected women: implications for HIV shedding. *Sex*
591 *Transm Infect*. 2004;80(2):108-112. doi:10.1136/sti.2003.005157

592 17. Gardella B, Roccio M, Maccabruni A, et al. HIV shedding in cervico-vaginal secretions in
593 pregnant women. *Curr HIV Res*. 2011;9(5):313-320. doi:Abs: CHIVR-162 [pii]

594 18. Seaton KE, Ballweber L, Lan A, et al. HIV-1 specific IgA detected in vaginal secretions of HIV
595 uninfected women participating in a microbicide trial in Southern Africa are primarily
596 directed toward gp120 and gp140 specificities. *PLoS One*. 2014;9(7).
597 doi:10.1371/journal.pone.0101863

598 19. Ghosh M, Fahey J V., Shen Z, et al. Anti-HIV activity in cervical-vaginal secretions from HIV-
599 Positive and -Negative women correlate with innate antimicrobial levels and IgG antibodies.
600 *PLoS One*. 2010;5(6). doi:10.1371/journal.pone.0011366

601 20. Clemetson DB, Moss GB, Willerford DM, et al. Detection of HIV DNA in cervical and vaginal
602 secretions. Prevalence and correlates among women in Nairobi, Kenya. *Jama*.
603 1993;269(22):2860-2864. doi:10.1016/0020-7292(94)90090-6

604 21. Burgener A, Rahman S, Ahmad R, et al. Comprehensive proteomic study identifies serpin and
605 cystatin antiproteases as novel correlates of HIV-1 resistance in the cervicovaginal mucosa of
606 female sex workers. *J Proteome Res*. 2011;10(11):5139-5149. doi:10.1021/pr200596r

607 22. Drannik AG, Nag K, Yao XD, et al. Anti-HIV-1 Activity of Elafin Depends on Its Nuclear
608 Localization and Altered Innate Immune Activation in Female Genital Epithelial Cells. *PLoS*
609 *One*. 2012;7(12). doi:10.1371/journal.pone.0052738

610 23. Yáñez-Mó M, Siljander PR-M, Andreu Z, et al. Biological properties of extracellular vesicles
611 and their physiological functions. *J Extracell vesicles*. 2015;4:27066. doi:10.3402/jev.v4.27066

612 24. Théry C, Witwer KW, Aikawa E, et al. Minimal information for studies of extracellular vesicles
613 2018 (MISEV2018): a position statement of the International Society for Extracellular Vesicles
614 and update of the MISEV2014 guidelines. *J Extracell Vesicles*. 2018;7(1).

615 doi:10.1080/20013078.2018.1535750

616 25. Witwer KW, Théry C. Extracellular vesicles or exosomes? On primacy, precision, and
617 popularity influencing a choice of nomenclature. *J Extracell Vesicles*. 2019;8(1):1648167.
618 doi:10.1080/20013078.2019.1648167

619 26. Meehan B, Rak J, Di Vizio D. Oncosomes - large and small: what are they, where they came
620 from? *J Extracell vesicles*. 2016;5:33109.

621 27. György B, Hung ME, Breakefield XO, Leonard JN. Therapeutic applications of extracellular
622 vesicles: clinical promise and open questions. *Annu Rev Pharmacol Toxicol*. 2015;55:439-464.
623 doi:10.1146/annurev-pharmtox-010814-124630

624 28. Witwer KW, Buzás EI, Bemis LT, et al. Standardization of sample collection, isolation and
625 analysis methods in extracellular vesicle research. *J Extracell vesicles*. 2013;2:1-25.
626 doi:10.3402/jev.v2i0.20360

627 29. Smith JA, Daniel R. Human vaginal fluid contains exosomes that have an inhibitory effect on
628 an early step of the HIV-1 life cycle. *AIDS*. August 2016. doi:10.1097/QAD.0000000000001236

629 30. Muth DC, McAlexander MA, Ostrenga LJ, et al. Potential role of cervicovaginal extracellular
630 particles in diagnosis of endometriosis. *Bmc Vet Res*. 2015. doi:10.1186/s12917-015-0513-7

631 31. Sergeeva AM, Pinzon Restrepo N, Seitz H. Quantitative aspects of RNA silencing in
632 metazoans. *Biochem*. 2013;78(6):613-626. doi:10.1134/S0006297913060072BCM78060795 [pii]

633 32. Bartel DP. MicroRNAs: target recognition and regulatory functions. *Cell*. 2009;136(2):215-233.
634 doi:S0092-8674(09)00008-7 [pii]10.1016/j.cell.2009.01.002

635 33. Valadi H, Ekström K, Bossios A, Sjöstrand M, Lee JJ, Lötvall JO. Exosome-mediated transfer
636 of mRNAs and microRNAs is a novel mechanism of genetic exchange between cells. *Nat Cell*
637 *Biol*. 2007;9(6):654-659. doi:10.1038/ncb1596

638 34. Aliotta JM, Sanchez-Guijo FM, Dooner GJ, et al. Alteration of marrow cell gene expression,
639 protein production, and engraftment into lung by lung-derived microvesicles: a novel
640 mechanism for phenotype modulation. *Stem Cells*. 2007;25(9):2245-2256.
641 doi:10.1634/stemcells.2007-0128

642 35. Baj-Krzyworzeka M, Szatanek R, Węglarczyk K, et al. Tumour-derived microvesicles carry
643 several surface determinants and mRNA of tumour cells and transfer some of these
644 determinants to monocytes. *Cancer Immunol Immunother*. 2006;55(7):808-818.
645 doi:10.1007/s00262-005-0075-9

646 36. Mateescu B, Kowal EJK, van Balkom BWM, et al. Obstacles and opportunities in the functional
647 analysis of extracellular vesicle RNA - an ISEV position paper. *J Extracell vesicles*.
648 2017;6(1):1286095. doi:10.1080/20013078.2017.1286095

649 37. Turchinovich A, Weiz L, Langheinz A, Burwinkel B. Characterization of extracellular
650 circulating microRNA. *Nucleic Acids Res*. 2011;39(16):7223-7233. doi:gkr254
651 [pii]10.1093/nar/gkr254

652 38. Arroyo JD, Chevillet JR, Kroh EM, et al. Argonaute2 complexes carry a population of
653 circulating microRNAs independent of vesicles in human plasma. *Proc Natl Acad Sci U S A*.
654 2011;108(12):5003-5008. doi:1019055108 [pii]10.1073/pnas.1019055108

655 39. Witwer KW, Sarbanes SL, Liu J, Clements JE. A plasma microRNA signature of acute lentiviral
656 infection: biomarkers of CNS disease. *AIDS*. 2011;204(7):1104-1114.
657 doi:10.1097/QAD.0b013e32834b95bf

658 40. Zubakov D, Boersma AW, Choi Y, van Kuijk PF, Wiemer EA, Kayser M. MicroRNA markers
659 for forensic body fluid identification obtained from microarray screening and quantitative RT-
660 PCR confirmation. *Int J Leg Med*. 2010;124(3):217-226. doi:10.1007/s00414-009-0402-3

661 41. Seashols-Williams S, Lewis C, Calloway C, et al. High-throughput miRNA sequencing and
662 identification of biomarkers for forensically relevant biological fluids. *Electrophoresis*. August
663 2016. doi:10.1002/elps.201600258

664 42. Rahman S, Rabbani R, Wachihi C, et al. Mucosal serpin A1 and A3 levels in HIV highly
665 exposed sero-negative women are affected by the menstrual cycle and hormonal
666 contraceptives but are independent of epidemiological confounders. *Am J Reprod Immunol*.
667 2013;69(1):64-72. doi:10.1111/aji.12014

668 43. Thery C, Amigorena S, Raposo G, Clayton A. Isolation and characterization of exosomes from
669 cell culture supernatants and biological fluids. *Curr Protoc Cell Biol*. 2006;Chapter 3:Unit 3 22.
670 doi:10.1002/0471143030.cb0322s30

671 44. McAlexander MA, Phillips MJ, Witwer KW. Comparison of methods for miRNA extraction
672 from plasma and quantitative recovery of RNA from cerebrospinal fluid. *Front Genet*.
673 2013;4(MAY):83. doi:10.3389/fgene.2013.00083

674 45. Chen C, Ridzon DA, Broomer AJ, et al. Real-time quantification of microRNAs by stem-loop
675 RT-PCR. *Nucleic Acids Res*. 2005;33(20):e179. doi:33/20/e179 [pii]10.1093/nar/gni178

676 46. Witwer KW, Sarbanes SL, Liu J, Clements JE. A plasma microRNA signature of acute lentiviral
677 infection: biomarkers of central nervous system disease. *AIDS*. 2011;25(17):2057-2067.
678 doi:10.1097/QAD.0b013e32834b95bf

679 47. Clough E, Barrett T. The Gene Expression Omnibus Database. *Methods Mol Biol*. 2016;1418:93-
680 110. doi:10.1007/978-1-4939-3578-9_5

681 48. Van Deun J, Mestdagh P, Agostinis P, et al. EV-TRACK: transparent reporting and
682 centralizing knowledge in extracellular vesicle research. *Nat Methods*. 2017;14(3):228-232.
683 doi:10.1038/nmeth.4185

684 49. Biton M, Levin A, Slyper M, et al. Epithelial microRNAs regulate gut mucosal immunity via
685 epithelium–T cell crosstalk. *Nat Immunol*. 2011;12(3):239-246. doi:10.1038/ni.1994

686 50. Jurcevic S, Olsson B, Klinga-Levan K. MicroRNA expression in human endometrial
687 adenocarcinoma. *Cancer Cell Int*. 2014;14(1):1-8. doi:10.1186/s12935-014-0088-6

688 51. Jayaraman M, Radhakrishnan R, Mathews CA, et al. Identification of novel diagnostic and
689 prognostic miRNA signatures in endometrial cancer. *Genes Cancer*. 2017;8(5-6):566-576.
690 doi:10.18632/genesandcancer.144

691 52. Cosar E, Mamillapalli R, Ersoy GS, Cho SY, Seifer B, Taylor HS. Serum microRNAs as
692 diagnostic markers of endometriosis: a comprehensive array-based analysis. *Fertil Steril*.
693 2016;106(2):402-409. doi:10.1016/j.fertnstert.2016.04.013

694 53. Schwarzenbach H, da Silva AM, Calin G, Pantel K. Data Normalization Strategies for
695 MicroRNA Quantification. *Clin Chem*. 2015;61(11):1333-1342.
696 doi:10.1373/clinchem.2015.239459

697 54. Nguyen HPT, Simpson RJ, Salamonsen LA, Greening DW. Extracellular Vesicles in the
698 Intrauterine Environment: Challenges and Potential Functions. *Biol Reprod*. 2016;95(5):109-
699 109. doi:10.1095/biolreprod.116.143503

700 55. Campoy I, Lanau L, Altadill T, et al. Exosome-like vesicles in uterine aspirates: a comparison
701 of ultracentrifugation-based isolation protocols. *J Transl Med*. 2016;14(1):180.
702 doi:10.1186/s12967-016-0935-4

703 56. Zegels G, Aa G, Raemdonck V, et al. Comprehensive proteomic analysis of human cervical-
704 vaginal fluid using colposcopy samples. *Proteome Sci*. 2009;7(7). doi:10.1186/1477-5956-7-17

705 57. Gravett MG, Thomas A, Schneider KA, et al. PROTEOMIC ANALYSIS OF CERVICAL-
706 VAGINAL FLUID: IDENTIFICATION OF NOVEL BIOMARKERS FOR DETECTION OF
707 INTRA-AMNIOTIC INFECTION. doi:10.1021/pr060149v

708 58. Arroyo JD, Chevillet JR, Kroh EM, et al. Argonaute2 complexes carry a population of
709 circulating microRNAs independent of vesicles in human plasma. *Proc Natl Acad Sci U S A*.
710 2011;108(12):5003-5008. doi:10.1073/pnas.1019055108

711 59. Guo Z, Maki M, Ding R, Yang Y, Zhang B, Xiong L. Genome-wide survey of tissue-specific
712 microRNA and transcription factor regulatory networks in 12 tissues. *Sci Rep*. 2014;4:1-9.
713 doi:10.1038/srep05150

714 60. Panwar B, Omenn GS, Guan Y. miRmine: A Database of Human miRNA Expression Profiles.
715 *Bioinformatics*. 2017;33(10):btx019. doi:10.1093/bioinformatics/btx019

716 61. Pritchard CC, Kroh E, Wood B, et al. Blood cell origin of circulating microRNAs: a cautionary
717 note for cancer biomarker studies. *Cancer Prev Res*. 2012;5(3):492-497. doi:1940-6207.CAPR-11-
718 0370 [pii]10.1158/1940-6207.CAPR-11-0370

719 62. Luo P, Wang Q, Ye Y, et al. MiR-223-3p functions as a tumor suppressor in lung squamous
720 cell carcinoma by miR-223-3p-mutant p53 regulatory feedback loop. *J Exp Clin Cancer Res*.
721 2019;38(1). doi:10.1186/s13046-019-1079-1

722 63. Ji Q, Xu X, Song Q, et al. miR-223-3p Inhibits Human Osteosarcoma Metastasis and
723 Progression by Directly Targeting CDH6. *Mol Ther*. 2018;26:1299-1312.
724 doi:10.1016/j.ymthe.2018.03.009

725 64. Lawrence M JY. miR-203 Functions as a Tumor Suppressor by Inhibiting Epithelial to
726 Mesenchymal Transition in Ovarian Cancer. *J Cancer Sci Ther*. 2015;07(02). doi:10.4172/1948-
727 5956.1000322

728 65. Deng B, Wang B, Fang J, et al. MiRNA-203 suppresses cell proliferation, migration and
729 invasion in colorectal cancer via targeting of EIF5A2. *Sci Rep*. 2016;6. doi:10.1038/srep28301

730 66. Wang S, Zhang R, Claret FX, Yang H. Involvement of microRNA-24 and DNA methylation in
731 resistance of nasopharyngeal carcinoma to ionizing radiation. *Mol Cancer Ther*.
732 2014;13(12):3163-3174. doi:10.1158/1535-7163.MCT-14-0317

733 67. Fang ZH, Wang SL, Zhao JT, et al. MIR-150 exerts antileukemia activity in vitro and in vivo
734 through regulating genes in multiple pathways. *Cell Death Dis*. 2016;7(9).
735 doi:10.1038/cddis.2016.256

736 68. Ito M, Teshima K, Ikeda S, et al. MicroRNA-150 inhibits tumor invasion and metastasis by
737 targeting the chemokine receptor CCR6, in advanced cutaneous T-cell lymphoma. *Blood*.
738 2014;123(10):1499-1511. doi:10.1182/blood-2013-09-527739

739 69. Huang J, Wang F, Argyris E, et al. Cellular microRNAs contribute to HIV-1 latency in resting
740 primary CD4+ T lymphocytes. *Nat Med*. 2007;13(10):1241-1247. doi:nm1639
741 [pii]10.1038/nm1639

742 70. Swaminathan S, Murray DD, Kelleher AD. miRNAs and HIV: unforeseen determinants of
743 host-pathogen interaction. *Immunol Rev*. 2013;254(1):265-280. doi:10.1111/imr.12077

744 71. Sisk JM, Witwer KW, Tarwater PM, Clements JE. SIV replication is directly downregulated by
745 four antiviral miRNAs. *Retrovirology*. 2013;10(1):95. doi:1742-4690-10-95 [pii]10.1186/1742-
746 4690-10-95

747 72. Wang X, Ye L, Zhou Y, Liu MQ, Zhou DJ, Ho WZ. Inhibition of anti-HIV microRNA
748 expression: a mechanism for opioid-mediated enhancement of HIV infection of monocytes.
749 *Am J Pathol*. 2011;178(1):41-47. doi:S0002-9440(10)00089-1 [pii]10.1016/j.ajpath.2010.11.042

750 73. Swaminathan S, Suzuki K, Seddiki N, et al. Differential regulation of the Let-7 family of
751 microRNAs in CD4+ T cells alters IL-10 expression. *J Immunol*. 2012;188(12):6238-6246.
752 doi:jimmunol.1101196 [pii]10.4049/jimmunol.1101196

753 74. Klase Z, Kale P, Winograd R, et al. HIV-1 TAR element is processed by Dicer to yield a viral

754 micro-RNA involved in chromatin remodeling of the viral LTR. *BMC Mol Biol*. 2007;8:63.
755 doi:1471-2199-8-63 [pii]10.1186/1471-2199-8-63

756 75. Wagschal A, Rousset E, Basavarajaiah P, et al. Microprocessor, Setx, Xrn2, and Rrp6 co-operate
757 to induce premature termination of transcription by RNAPII. *Cell*. 2012;150(6):1147-1157.
758 doi:10.1016/j.cell.2012.08.004S0092-8674(12)00999-3 [pii]

759 76. Whisnant AW, Bogerd HP, Flores O, et al. In-Depth Analysis of the Interaction of HIV-1 with
760 Cellular microRNA Biogenesis and Effector Mechanisms. *MBio*. 2013;4(2).
761 doi:10.1128/mBio.00193-13e00193-13 [pii]mBio.00193-13 [pii]

762 77. Sung TL, Rice AP. miR-198 inhibits HIV-1 gene expression and replication in monocytes and
763 its mechanism of action appears to involve repression of cyclin T1. *PLoS Pathog*.
764 2009;5(1):e1000263. doi:10.1371/journal.ppat.1000263

765 78. Hsu SD, Tseng YT, Shrestha S, et al. miRTarBase update 2014: an information resource for
766 experimentally validated miRNA-target interactions. *Nucleic Acids Res*. 2014;42(Database
767 issue):D78-85. doi:10.1093/nar/gkt1266

768 79. Hsu SD, Lin FM, Wu WY, et al. miRTarBase: a database curates experimentally validated
769 microRNA-target interactions. *Nucleic Acids Res*. 2011;39(Database issue):D163-9.
770 doi:10.1093/nar/gkq1107

771 80. Vergoulis T, Vlachos IS, Alexiou P, et al. TarBase 6.0: capturing the exponential growth of
772 miRNA targets with experimental support. *Nucleic Acids Res*. 2011. doi:gkr1161
773 [pii]10.1093/nar/gkr1161

774 81. Vlachos IS, Paraskevopoulou MD, Karagkouni D, et al. DIANA-TarBase v7.0: indexing more
775 than half a million experimentally supported miRNA:mRNA interactions. *Nucleic Acids Res*.
776 2015;43(Database issue):D153-9. doi:10.1093/nar/gku1215

777 82. Lagana A, Forte S, Giudice A, et al. miRo: a miRNA knowledge base. *Database*.
778 2009;2009(0):bap008-bap008. doi:10.1093/database/bap008

779 83. Papadopoulos GL, Alexiou P, Maragkakis M, Reczko M, Hatzigeorgiou AG. DIANA-mirPath:
780 Integrating human and mouse microRNAs in pathways. *Bioinformatics*. 2009;25(15):1991-1993.
781 doi:10.1093/bioinformatics/btp299

782 84. Vlachos IS, Zagganas K, Paraskevopoulou MD, et al. DIANA-miRPath v3.0: deciphering
783 microRNA function with experimental support. *Nucleic Acids Res*. 2015;43(W1):W460-W466.
784 doi:10.1093/nar/gkv403

785 85. Myatt SS, Wang J, Monteiro LJ, et al. Definition of microRNAs that repress expression of the
786 tumor suppressor gene FOXO1 in endometrial cancer. *Cancer Res*. 2010;70(1):367-377.
787 doi:10.1158/0008-5472.CAN-09-1891

788 86. Zhou L, Qi X, Potashkin JA, Abdul-Karim FW, Gorodeski GI. MicroRNAs miR-186 and miR-

789 150 down-regulate expression of the pro-apoptotic purinergic P2X7 receptor by activation of
790 instability sites at the 3′-untranslated region of the gene that decrease steady-state levels of
791 the transcript. *J Biol Chem*. 2008;283(42):28274-28286. doi:10.1074/jbc.M802663200

792 87. Niinuma T, Kai M, Kitajima H, et al. Downregulation of miR-186 is associated with metastatic
793 recurrence of gastrointestinal stromal tumors. *Oncol Lett*. 2017;14(5):5703-5710.
794 doi:10.3892/ol.2017.6911

795 88. Paraskevopoulou MD, Vlachos IS, Hatzigeorgiou AG. DIANA-TarBase and DIANA Suite
796 Tools: Studying Experimentally Supported microRNA Targets. *Curr Protoc Bioinforma*.
797 2016;55(1):12.14.1-12.14.18. doi:10.1002/cpbi.12

798 89. Ji Diana Lee Y, Kim V, Muth DC, Witwer KW. Validated MicroRNA Target Databases: An
799 Evaluation. *Drug Dev Res*. 2015;76(7):389-396. doi:10.1002/ddr.21278

800 90. Gardiner C, Vizio D Di, Sahoo S, et al. Techniques used for the isolation and characterization
801 of extracellular vesicles: results of a worldwide survey. *J Extracell Vesicles*. 2016;5(0).
802 doi:10.3402/jev.v5.32945

803 91. Witwer KW, Halushka MK. Towards the Promise of microRNAs - Enhancing reproducibility
804 and rigor in microRNA research. *RNA Biol*. September 2016:0.
805 doi:10.1080/15476286.2016.1236172

806 92. La Rocca G, Olejniczak SH, Gonzalez AJ, et al. In vivo, Argonaute-bound microRNAs exist
807 predominantly in a reservoir of low molecular weight complexes not associated with mRNA.
808 *Proc Natl Acad Sci U S A*. 2015;112(3):767-772. doi:10.1073/pnas.1424217112

809

SUPPLEMENTAL MATERIALS

Supplemental Figure S1. Collection Materials and Workflow

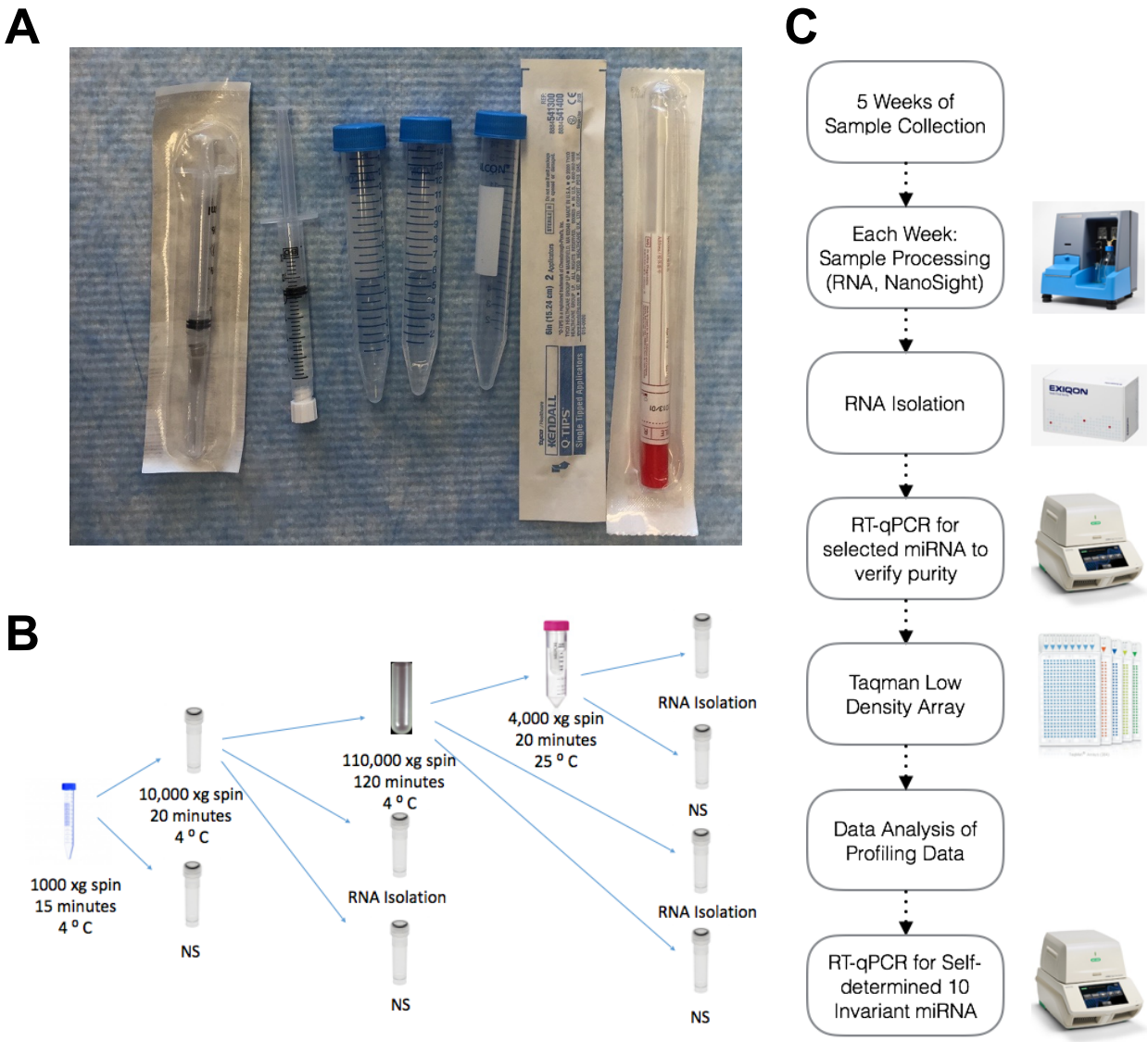

Supplemental Figure S2

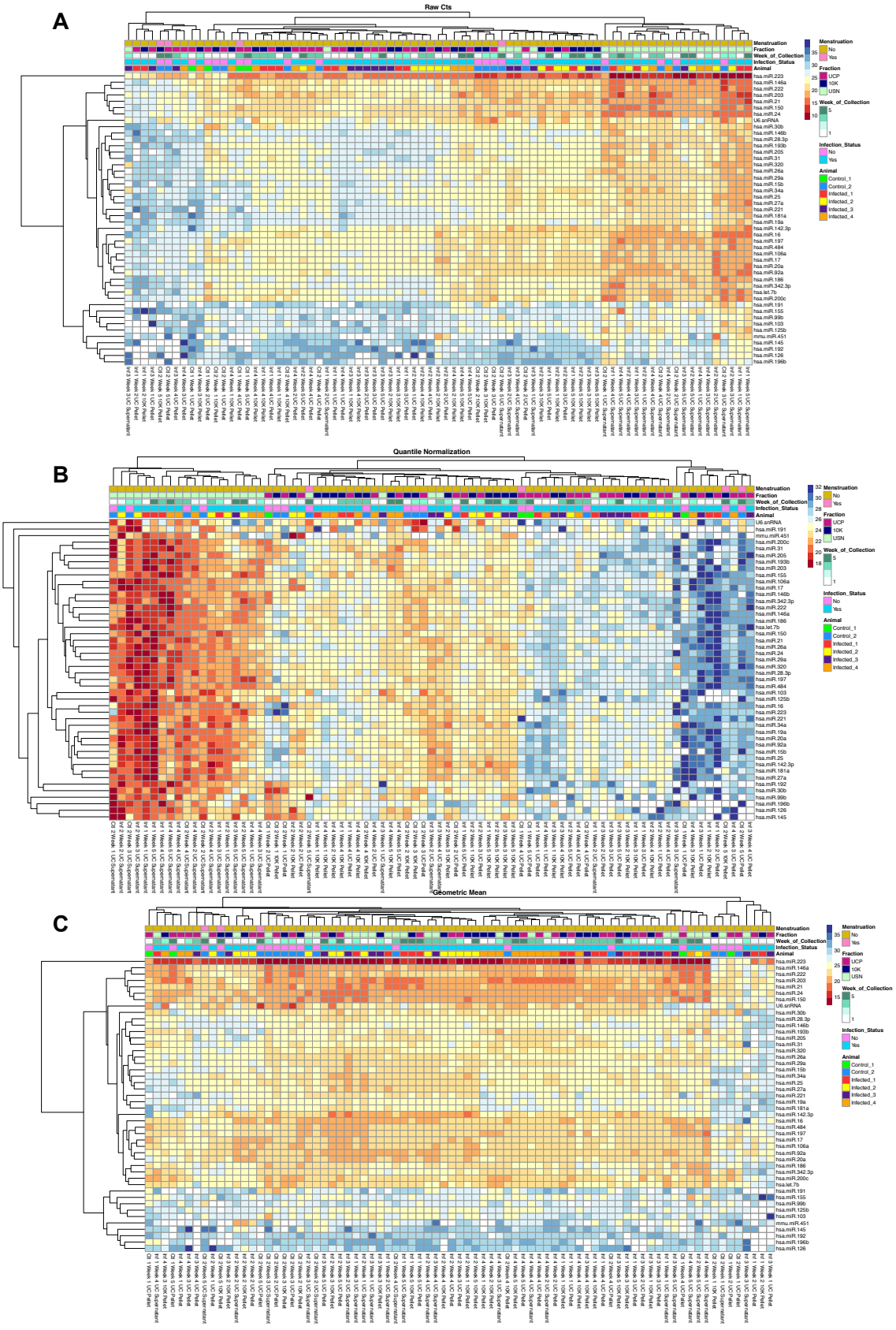

816 **SUPPLEMENTAL TABLES**

817 **Supplemental Table 1. Recovered volumes: CVL**

Subject	Week 1	Week 2	Week 3	Week 4	Week 5
Control 1	1 mL	2 mL	1 mL	1 mL	1 mL
Control 2	3 mL	0.7 mL	2 mL	0.5 mL	1.25 mL
Infected 1	1 mL	0.2 mL	0.5 mL	0.3 mL	1.5 mL
Infected 2	1.5 mL	1.5 mL	2 mL	0.8 mL	1.75 mL
Infected 3	0.5 mL	0.6 mL	2.8 mL	0.8 mL	2 mL
Infected 4	0.8 mL	0.3 mL	0.6 mL	0.3 mL	1.5 mL

818
819

820 **Supplemental Table 2. NTA dilution factors, CVL**

	Time point	Subject					
		Control 1	**Control 2**	**Infected 1**	**Infected 2**	**Infected 3**	**Infected 4**
CVL (UC Supernatant)	Week 1	1:25	1:50	1:25	1:25	1:25	1:25
	Week 2	1:100	1:5	1:25	1:10	1:5	1:5
	Week 3	1:10	1:5	1:5	1:5	1:10	1:10
	Week 4	1:10	1:5	1:10	1:5	1:10	1:10
	Week 5	1:5	1:10	1:10	1:10	1:5	1:5
CVL (UC Pellet)	Week 1	Neat	1:5	1:5	1:5	1:5	1:5
	Week 2	1:10	1:10	1:5	1:5	1:5	1:5
	Week 3	1:5	1:5	1:5	1:5	1:5	1:5
	Week 4	1:5	1:5	1:5	1:5	1:5	1:5
	Week 5	1:5	1:5	1:5	1:5	1:5	1:5

Abbreviations: CVL = cervicovaginal lavage; UC = ultracentrifugation

821

822 **Supplemental Table 3. Pooling strategy: Western blot**

823

Pool 1 (healthy and infected)	Healthy 2 Week 5, Infected 1 Week 2, Infected 3 Week 2, Infected 3 Week 5, Infected 2 Week 3, Infected 2 Week 4
Pool 2 (all healthy)	Healthy 1 Week 4, Healthy 1 Week 5, Healthy 2 Week 2, Healthy 2 Week 3, Healthy 2 Week 4, Healthy 1 Week 2
Pool 3 (all infected)	Infected 5 Week 2, Infected 3 Week 3, Infected 2 Week 4, Infected 4 Week 5, Infected 4 Week 3, Infected 1 Week 5

824